www.sciencemag.org/cgi/content/full/316/5827/1054/DC1

Supporting Online Material for

Conformational Switching in the Fungal Light Sensor Vivid

Brian D. Zoltowski, Carsten Schwerdtfeger, Joanne Widom, Jennifer J. Loros, Alexandrine M. Bilwes, Jay C. Dunlap, Brian R. Crane*

*To whom correspondence should be addressed. E-mail: bc69@cornell.edu

Published 18 May 2007, *Science* **316**, 1054 (2007)
DOI: 10.1126/science.1137128

This PDF file includes:

Supplementary Information

Materials and Methods

A) Crystallography -

Crystallization

Monoclinic VVD-36 crystals of space group $P2_1$ were obtained for native, C71S, and phosphodiesterase treated VVD-36 (PDEVVD). VVD crystals have different forms depending on the dimensions of the a and c axes (Table S1). The larger unit cell contains 4 molecules per asymmetric unit, whereas the smaller contains two molecules per asymmetric unit (the same VVD dimer is common to all lattices and molecular packing arrangements are similar for each). Crystals were grown overnight at 22 °C under constant darkness by vapor diffusion from 8 mg/mL protein. Crystals will not form in the light state, except for C71S. Crystals grew from an equal volume (2 L) of protein dissolved in a buffer containing 50 mM HEPES pH 8.0, 150 mM NaCl and 13% glycerol, and a reservoir solution containing 100 mM tri-sodium citrate pH 5.6, 100 mM ammonium acetate and 30% PEG 5K MME. The largest crystals appear as single plates (500 m x 500 m x 10 m) that diffract to between 1.7 - 2.3 Å resolution.

Crystal Spectroscopy

Photobleaching of crystals was monitored by a custom-built microspectrophotometer coupled to a 75W Xe-arc lamp (*1-4*). Single crystals were mounted in flat wall slides or capillaries and irradiated with visible light (400-600 nm) focused by reflecting optics to the facial profile of the crystal (diameter = ~0.1-0.3 m). Light passing through the crystals were collected in fiber optics, dispersed on a 600 lines/mm grating and recorded by a 2048-element linear silicon CCD array (Ocean Optics). Crystals bleach rapidly ($t_{1/2}$ = ~ < 1 sec) at light intensities necessary for a measurable transmittance (effective protein concentration in the crystals ~ 50 mM). Incident light intensities that gave an acceptable absorption spectra but also allowed resolution of the bleaching kinetics could not exceed ~ 0.1 W integrated over the VVD visible absorption band (400-550 nm), as measured by a calibrated photon counting CCD. Even

under these intensities, it is impossible to collect enough light through the crystal in the time necessary to trap a fully dark state spectrum. Approximately 30% conversion occurs within 300 msec (Fig. S3). Importantly, photobleaching of the crystals was entirely reversible, with full recovery occurring on approximately the same time scale as observed in solution ($t_{1/2}$ = 3 hr). Once bleached, crystals appear clear in color; and if cooled to 100 K do not recover the dark-sate spectrum. These color differences could be observed directly and confirmed on the CCD cameras at the synchrotron beam-lines. To ensure that the "dark-state" structures were not light excited, crystals were grown in the dark; and flash cooled under dim red light. Test crystals were examined in the light after this procedure and observed to be completely yellow. Nevertheless, diffraction data were collected in the dark. The reducing effect of the synchrotron beam on the redox state of VVD was also readily observed by the crystal CCD images.

Structure Determination and Refinement

Diffraction data was collected at 100 K with synchrotron radiation on beamline X-29 (dark state VVD and PDEVVD), and X-24 (light state VVD) at the National Synchrotron Light Source (NSLS) at Brookhaven National laboratory. VVD C71S mutant data was collected at beamline F1 at the Cornell High Energy Synchrotron Source (CHESS). The data was reduced and scaled with HKL2000 (*5*) (Table A1). Initial phases for dark state VVD were obtained by molecular replacement (MR) AmoRe (*6*) using the phototropin PHY3-LOV2 structure (PDB ID 1g28) as a search model. Additional phases for other structures were obtained with dark state VVD as a molecular replacement probe. The models were subsequently rebuilt using XFIT(*7*) and F_{obs}-F_{calc} and $2F_{obs}$-F_{calc} maps. Simulated-annealing of the initial MR solution did not improve the initial electron density maps and hence was not used in the structure determination. Several rounds of rebuilding were followed by refinement in CNS (*8*) using standard positional and thermal factor refinement. Omit and difference maps were prepared with XtalView (*7*). The flavin was left out of the molecular replacement probe and added only at the later stages of refinement. The quality of the flavin

electron density was used as a metric for improvement of the model throughout the refinement procedure. Light-adapted data sets were collected by exposing crystals to a high intensity broad spectrum light source for 2 minutes prior to cryo-cooling in the cold stream at the X-Ray source. Spectral changes corresponding to formation of the light adapted state correlated with the crystals turned from yellow to clear and bleaching was fully reversible (Fig. S3). It was determined the X-ray beam reduced the covalent adduct formed in light-adapted VVD-36, therefore only early frames were useful for obtaining a light-state structure. Such X-ray mediated reduction of the flavin adduct was also encountered with the Phot-LOV1 domain from *C. reinhardtii (9)*. To obtain a complete data set of light-adapted VVD-36 the first 30 frames of four data sets were merged with HKL2000. The resulting structure was obtained analogous to the method used for dark-adapted VVD-36. Even under these conditions, the light state is not fully populated in the crystal and two of the molecules in the asymmetric unit have a higher proportion of the adduct than the other two. Both dark and light state conformations were refined in each molecule and the relative occupancies determined by manual adjustment followed by examination of residual peaks in the difference Fourier maps. This method indicated that two of the molecules contain approximately ~60% of the light state, whereas the other two contain only ~40%. Importantly, all molecules show adduct formation, movement of Cys71 and the shift in b (Figs. S3 and S4). None of these features are found in the dark state structures of the WT or the Cys71Ser mutant. If Gln182 is modeled as only the unflipped dark-state conformation, difference peaks reflecting exchange of the O and N atoms of the amide appear in only the two molecules with the highest adduct occupancy. We examined all other Asn and Gln residues in the four structures and found that no others had similar patterns of difference peaks. Furthermore, we purposely flipped the amides of other Gln and Asn residues and found that difference peaks indicative of the incorrect positions could be detected for only those that had low B-factors (this amounted to 21% of the amides in molecules 1 and 3 and 36% of the amides in molecules 2 and 4). Thus, it is not surprising that we can only distinguish the

Gln182 amide conformation in the molecules that have the highest population of the light state.

B) Small Angle X-ray Scattering -

Data Collection:

Small-angle X-ray scattering (SAXS) studies were performed at the G1 beamline of the Cornell High-Energy Synchrotron Source. Multilayer optics provided a 8.71 keV (1.42 Å) beam with 1% bandwidth. Slits were used to collimate the beam to 500 X 500 m diameter. A sample cell having path length of 1.5 mm was mounted in a small air gap between the slits and a vacuum flight path. Sample-to-detector distance was calibrated using a silver behenate powder sample and the known wavelength. Data were taken at ambient temperature and checked periodically for radiation-induced aggregation by comparison of successive scattering profiles. Samples of C71S, dark VVD-36, and light VVD-36 in 50 mM HEPES pH 8.0, 150 mM NaCl and 13% glycerol, were exposed at two concentrations 0.5 mg/ml and 5 mg/ml (C71S) and 0.8 mg/ml and 8 mg/ml (VVD-36). Dilute and concentrated samples of C71S and VVD-36 were subjected to identical exposure regimes consisting of four 5-second exposures, two 10-second exposures, and three 20-second exposures. Signal was recorded on a Quantum 1 detector (Area Detector Systems Corporation) and averaged to obtain radial intensity profiles.

Data Analysis

Profiles from matched buffer samples (same exposure time) were subtracted from protein solution profiles to yield final scattering curves. Pair distance distribution functions, Dmax (maximum dimension of the object), and Rg (radius of gyration) were calculated with GNOM (*10, 11*). Theoretical pairwise distribution function for the monomer and dimer, were obtained by generating scattering profiles from VVD PDB structures using CRYSOL (*12*). The resulting scattering curves were treated as data sets and the pair distance distribution functions, Dmax (maximum dimension of the object), and Rg (radius of gyration) were calculated in a manner analogous to the scattering curves obtained from SAXS. To monitor aggregation and radiation damage, Kratky plots were

generated ($I(Q)*Q^2$ vs. Q) where I(Q) is the scattering intensity and where Q=4 sin(/) is the momentum transfer. Kratky plots for all the systems indicated globular structures until after the first 20 second exposure, when increased $I(Q)*Q^2$ values at high Q indicated some denaturation. Thus, the latter 20 second exposures were excluded from data analysis. Furthermore, the value of I(Q) as Q 0, which is indicative of protein aggregation/dimerization, was determined to reflect globular monomeric species until longer time exposures, consistent with the Kratky plots. Crystallography studies indicated that X-ray sources deplete the light state conformation, thus to maximize the population of the light state species only the first 5 second exposure was used to determine the pairwise distribution for the light-adapted species. For mutant and dark-adapted VVD-36 the first 20 second and 10-second exposures were used to maximize signal-to-noise ratio, while minimizing radiation induced damage.

C) Biochemistry -

Mutagenesis

Cys71Ser, Cys71Ala, Cys71Val and Gln182Leu mutants were prepared by the QuickChange protocol (Stratagene) using the following primers. Cys71Ser 5'-CCT GTT GAC ACG TCA TCA GCT CTG ATT CTG TGC-3', 5'-GCA CAG AAT CAG AGC TGA TGA CGT GTC AAC AGG-3'. Cys71Ala 5'-CCT GTT GAC ACG TCA GCC GCT CTG ATT CTG TGC-3', 5'-GCA CAG AAT CAG AGC GGC TGA CGT GTC AAC AGG-3'. Cys71Val 5'-GAC ACG TCA GTC GCT CTG ATT CTG TGC GA-3', 5'-CAG AGC GAC TGA CGT GTC AAC AGG TCC C-3'. Gln182Leu 5'-TCA TTC CGT TTC GCA CAG GAA ACC CAT GCT GTA CCG-3', 5'-CGG TAC AGC ATG GGT TTC CTG TGC GAA ACG GAA TGA-3'. All mutated genes were sequenced in their entirety at the Biotechnology Resource Center of Cornell University.

Protein Expression and Purification

A VVD construct N-terminally truncated by 36 residues was PCR cloned into pet28 (Novagen) and overexpressed in E. coli BL21(DE3) cells. VVD-36 and its mutants (C71S, C71A, C71V, and Q182L) were induced with 100 M IPTG and expressed for 22 hours at 18 C under constant light. Proteins were first purified by Ni:NTA chromatography, prior to treatment with thrombin overnight. The protein was then purified on a Superdex 75 hi-load FPLC column and concentrated to 8 mg/mL for crystallization.

Size Exclusion Chromatography

Size exclusion chromatography was used to observe conformational changes after light excitation in VVD-36, PDEVVD, and the C71S, C71A, C71V and Q182L mutants. Dark state samples were purified and treated with thrombin overnight. Spectra were obtained on an Agilent 8453 spectrophotometer to verify 100% population of the dark state prior to injection unto a Superdex 75 HiLoad FPLC column equilibrated with buffer containing 50 mM HEPES pH 8.0, 150 mM NaCl and 13% glycerol. To generate the light-state, samples were incubated on ice in constant light (ambient light source) for 30 minutes prior to injection onto the FPLC. Spectra were obtained to verify population of the covalent adduct. The shift in hydrodynamic radii seen on light excitation is fully reversible for VVD-36, but less so with the Cys71Ala mutant, where a significant portion of the sample only appears to adopt the light state once.

Spectroscopy and Kinetics

All spectroscopy was conducted on an Agilent 8453 spectrophotometer. Kinetics of adduct recovery was determined by obtaining spectra at either 1 or 5 minute intervals for 10 hours. The resulting curves were fit using the exponential decay functions in Origin. VVD-36 adduct formation was achieved by incubating the protein on ice in constant light for 10 minutes. 100% population of the light state was verified by the absence of absorption bands at 428, 450 and 478 nm. Half

lives varied between 6-10 x 10^3 sec (k =1.0-1.7 x 10^{-4} s^{-1}) depending on the rate of sample acquisition, which affects repopulation of the light state by the light source.

D) *Neurospora* Studies -

Neurospora strains and growth conditions

Neurospora wild-type strain 74OR23-1A (FGSC 987) and the mutant vvd^{P4246} (FGSC 7854) were obtained from the Fungal Genetic Stock Center (Kansas City, KS). Growth of *Neurospora* was performed in Vogel's minimal medium supplemented with 1.5% sucrose in the dark (*13*). Mycelia were collected by filtration.

Production of vvd^{C71S} and vvd^{C76S} mutant strains

The genomic DNA construct used for complementation experiments in *N. crassa* contained a 6 His-tag and was constructed as described in (*14*). The complementation plasmid pCBCS108 was used to create the Cys71Ser and Cys76Ser mutant using the quick mutagenesis protocol adapted from Stratagene. The following oligonucleotides were used for the introduction of the mutation Cys71Ser: vvdCys71>S 5', CTG GGA CCT GTT GAC ACG TCA TCC GCT CTG ATT CTG TGC GAC CTG; vvd Cys71>S 3' GCT TCA GGT CGC ACA GAA TCA GAG CGG ATG ACG TGT CAA CAG G; Cys76Ser: vvd Cys76>S 5', CAT GCG CTC TGA TTC TGT CCG ACC TGA AGC AAA AAG ACA CGC C; vvd Cys76>S 3', GCT TCA GGT CGG ACA GAA TCA GAG CGC ATG ACG TGT CAA CAG G. The introduction of the mutation in both constructs (pCBCS109 and pCBCS110) was verified by DNA sequence analysis, respectively. The transformation of *Neurospora* was carried out by electroporation according to (*15*). Several transformants were isolated by at least three rounds of purifications and used for further analysis.

Purification of VVD protein

N. crassa cells were harvested and prepared as described in (*14*). The ground mycelia were resuspended in Lysate buffer for native protein purification according to the Qiagen protocol. After 2h binding in constant light @4 C elution was performed according to the Qiagen protocol.

Preparation of Neurospora and Western blot analysis

Western blot analysis was carried out as previously described in (*14*). For SDS/PAGE equal quantities of total cell lysates (~ 120 µg protein) or purified VVD protein were applied. In addition to protein quantifications, total cell lysates were separated on SDS gels and stained with Coomassie Blue prior to Western blot analysis to allow adjustment of protein concentrations. For the detection of VVD, proteins were separated on 17.5% SDS gels.

Further Tests to Rule Out Oligomerization in The Light-adapted State:

1) Cross Linking Assays

***Amine specific*:**

Light- and dark-state samples of VVD-36 at 8 mg/ml were diluted to 4 mg/ml with 10 mM DSP (Dithiobis[succinimidylpropionate]) dissolved in 50 mM HEPES pH8.0, 150 mM NaCl and 13% glycerol. Samples were incubated on ice for two hours prior to being quenched with 1.0 M Tris pH 7.5. The degree of cross-linking was determined via 12% Bis-Tris gel run with MOPS running buffer.

***Thiol specific*:**

Light- and dark-state samples of VVD-37 concentrated to 8 mg/ml was diluted to 1 mg/ml with 1 mM oxidized glutathione dissolved in 50 mM HEPES pH8.0, 150 mM NaCl and 13% glycerol. Samples were incubated on ice for 1-hour prior to transfer to SDS loading buffer for PAGE analysis. The degree of cross-linking was determined via 12% Bis-Tris gel run with MOPS running buffer.

***Glutaraldehyde*:**

All dilutions were made from a 1% stock solution of glutaraldehyde. Light- and dark-state samples of VVD-37 were prepared to a final concentration of 0.8 mg/ml. 5 l of 1% glutaraldehyde was added to 45 l of 0.8 mg/ml VVD-37 and incubated on ice and at 22 C. Samples were taken at 30 and 60 minutes and quenched with 1.0 M Tris pH 7.5. The degree of cross-linking was determined via 12% Bis-Tris gel run with MOPS running buffer.

In all cases, the amount of dimer and higher-molecular weight species increased with increasing time or concentration of cross-linking agents; however, under no circumstance was there a significantly different cross-linking pattern for light or dark state VVD (data not shown).

2) Engineered Cysteine Cross-linking:

Within the crystallographic VVD dimer Met55 on a contacts its symmetry mate. To probe whether the crystallographic dimer forms in solution under dark or light-state conditions, a Met55Cys substitution was introduced into a to allow for cysteine-mediated crosslinking. To facilitate crosslinking two oxidative conditions were used: copper phenanthroline and oxidized glutathione were added to 100 l of Met55Cys (8 mg/mL) to final concentrations of 1 mM and 10 mM respectively. The degree of cross-linking was determined by visual examination of bands on a 12% Bis-Tris SDS gel stained with Coomassie blue. The Met55Cys variant still undergoes the light-state conformational transition; however, no disulfide cross-linked dimer formed under normal or oxidative conditions, in either the dark or the light.

3) Limited Proteolysis

Limited proteolysis was conducted on both light-and dark-state VVD using proteinase K and trypsin. Purified VVD-36 was diluted to 0.8 mg/ml, then split into two fractions. One was treated with light for 10 minutes, whereas the other was stored on ice in the dark. After light/dark incubation 1:50, 1:100, and 1:500 mass ratio's of VVD to protease was added to both the light and the dark samples. Proteolysis was allowed to continue for 45-120 minutes, at which point

fractions were taken and added to SDS loading buffer. A 12% Bis-Tris Gel was run with MOPS running buffer to assay the extent of proteolysis in both the light- and dark-state samples. On average 5-6 noticeable fragments were present at the same molecular weight in both light- and dark-samples. Again, in no case was there a noticeable difference in the proteolytic degradation of light- compared to dark-state VVD.

Supplemental Figures

Supplemental Fig. S1. Secondary structure assignment and sequence alignment of VVD homologs

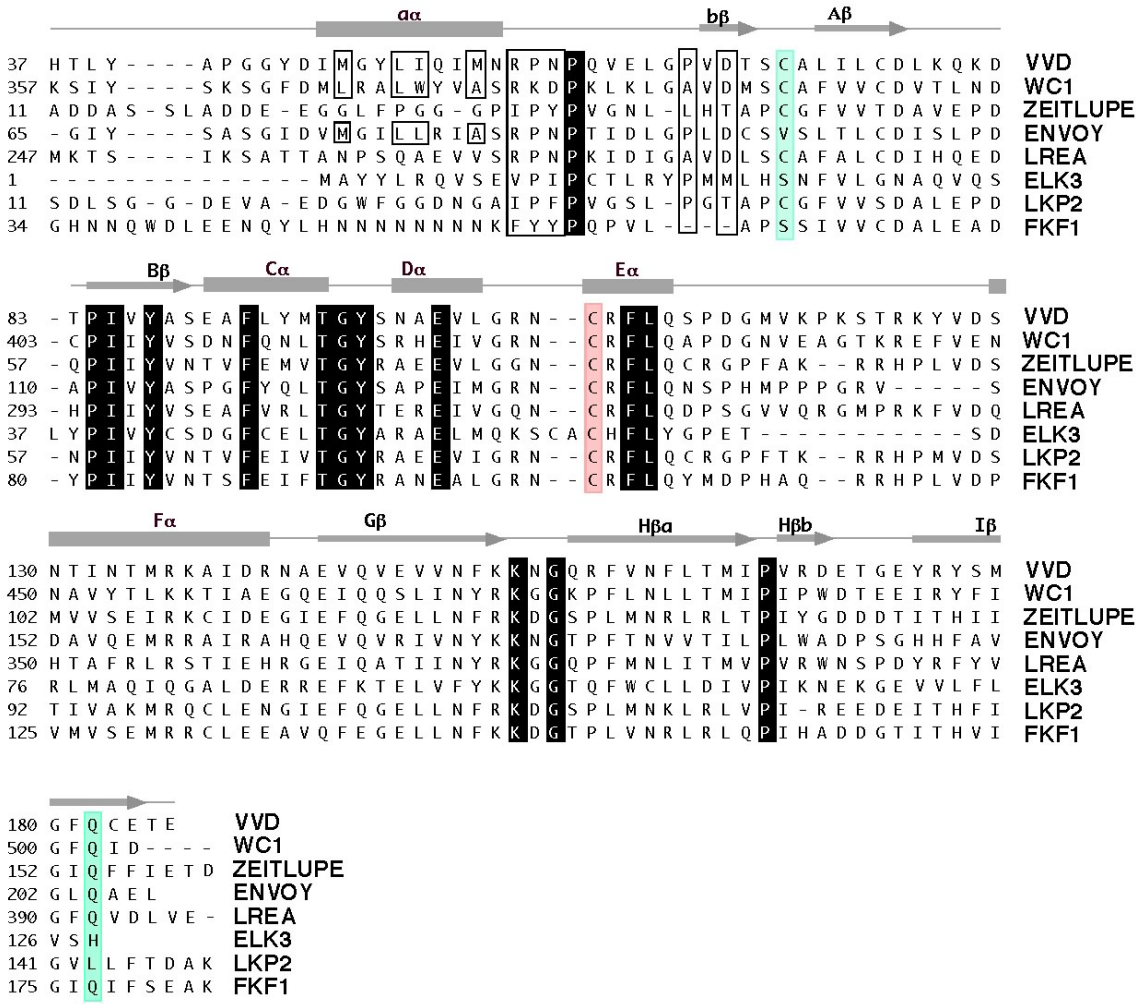

Sequence alignment of the LOV domains from *Neurospora crassa* VVD, *N. crassa* White-Collar 1 (WC1 XP_959777, the circadian clock transcription factor), ZEITLUPE (*Arabidopsis thaliana* NP_568855, an F-box protein involved in the plant clock), ENVOY (*Hypocrea jecorina* AAT40588, a fungal protein involved in light mediated expression of cellulase), LREA (XP_755026 a GATA transcription factor from *Aspergillus fumigatus*), ELK3 Ether-a-go-go-like potassium channel (ELK3 XP_700253, from *Danio rerio*), LKP2 (*Arabidopsis thaliana* NP_849983,

an F-box protein), and FKF1 (AAQ73528, an F-box protein involved in flowering regulation from *Mesembryanthemum crystallinum*).

Secondary structure elements of VVD shown in grey, invariant Cys108 highlighted in red, additional invariant residues in black, and the positions for Cys71 and Gln182 shown in green. Boxed residues in the N-terminal cap indicate the exposed hydrophobic face of a and conservation within the a b loop. All sequences conserve Cys108, including ELK3, which is not known to bind a flavin cofactor and does not function as a photoreceptor. Most sequences conserve Gln182, with the exception of ELK3, which has a His residue at this position. Key residues for flavin binding and PAS structural transitions are invariant (black). At position 71, Cys is well conserved, except in the more distant members, ELK3 and FKF1, where a Ser (non-functional in VVD) resides. As residues in the Asp68-Cys71 turn primarily interact with the Cys71 thiol through the peptide backbone, some substitutions are likely tolerated by the switching mechanism. Pro66 is reasonably well-conserved or substituted by similar residues (Ala, Leu). Greater variability is observed in the a helix, which may reflect coupling to different outputs.

Supplemental Fig. S2. Single Crystal Spectroscopy of VVD-36.

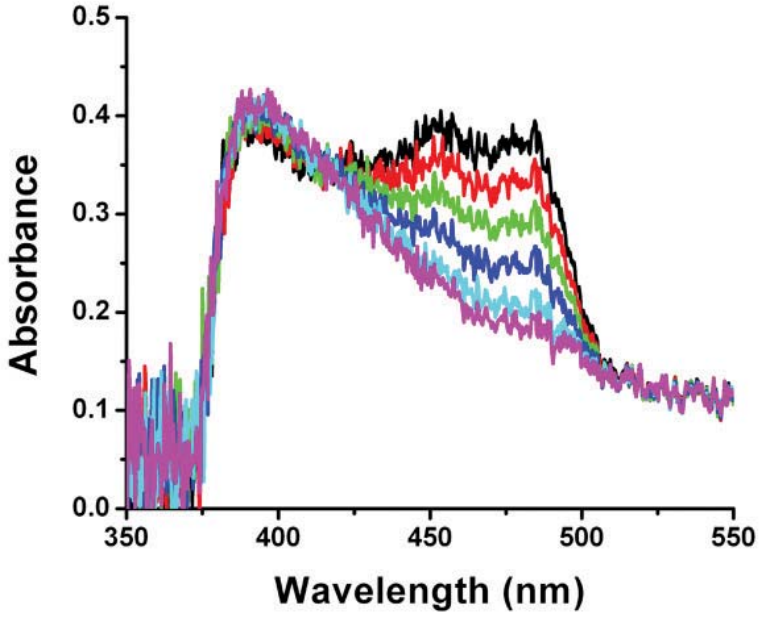

Spectra are shown at 0 sec (black), 0.6 sec (red), 1.5 sec (green), 3 sec (blue), 6 sec (aqua) and 9 sec (purple) after 0.1 W of 400-550 nm light exposure. Each spectrum represents the average of 10 scans, each integrated over 25 ms, and recorded every 300 ms. By the completion of the first exposure ~20% of the molecules have converted to the light-adapted state. The bleaching is reversible in the crystal, with the dark-state spectrum recovering in ~6 hrs.

Supplemental Fig. S3. Stereoviews of changes in the VVD active site. Overlay of light- (yellow) and dark-state (orange) VVD-36 active sites. Difference Fourier electron density maps (Fo-Fc) were calculated from structures refined with 100% of the dark state conformation. Difference map contours shown at +2.0 (aqua), +3.0 (blue), -2.0 (orange), and -3.0 (red). From top to bottom, molecule 1 (A), molecule 2 (B), molecue 3 (C) and molecule 4 (D). In the crystal, symmetric dimers form about a from molecules A and B, and molecules C and D. Note that in these difference maps, Fc does not contain contribution from the low-occupancy, alternate conformation of Cys108 (See Fig. 2A).

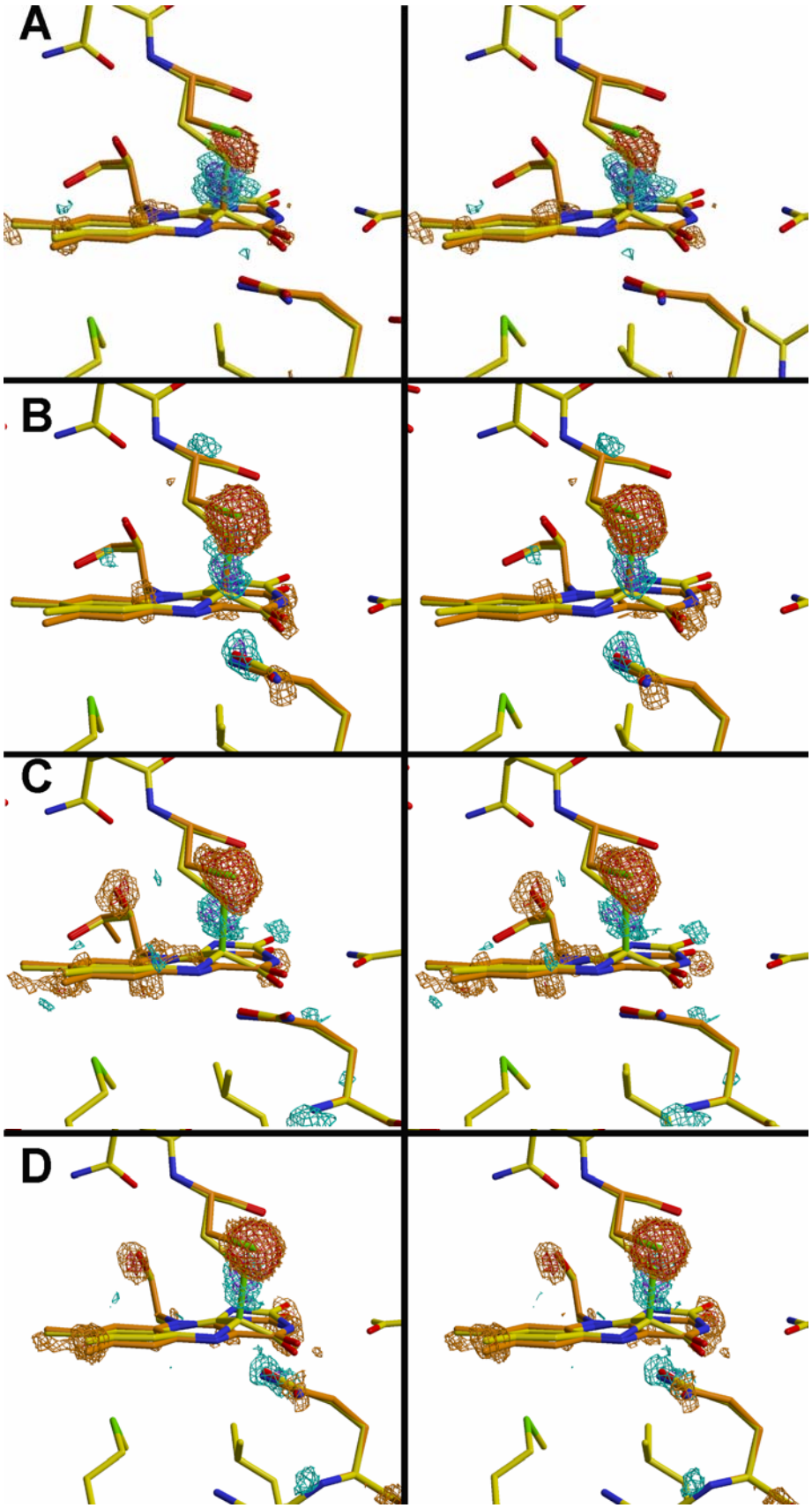
A
B
C
D

Supplementary Fig. S4. Stereoview of changes in the VVD-36 hinge region. Overlay of light- (yellow) and dark-state (orange) VVD hinge regions that correspond to the active sites shown in Fig S3. Contours are shown at +2.0 (aqua), +3.0 (blue), -2.0 (orange), and -3.0 (red). From top to bottom all four independent molecules in the asymmetric unit are shown molecule 1 (A), molecule 2 (B), molecule 3 (C) and molecule 4 (D).

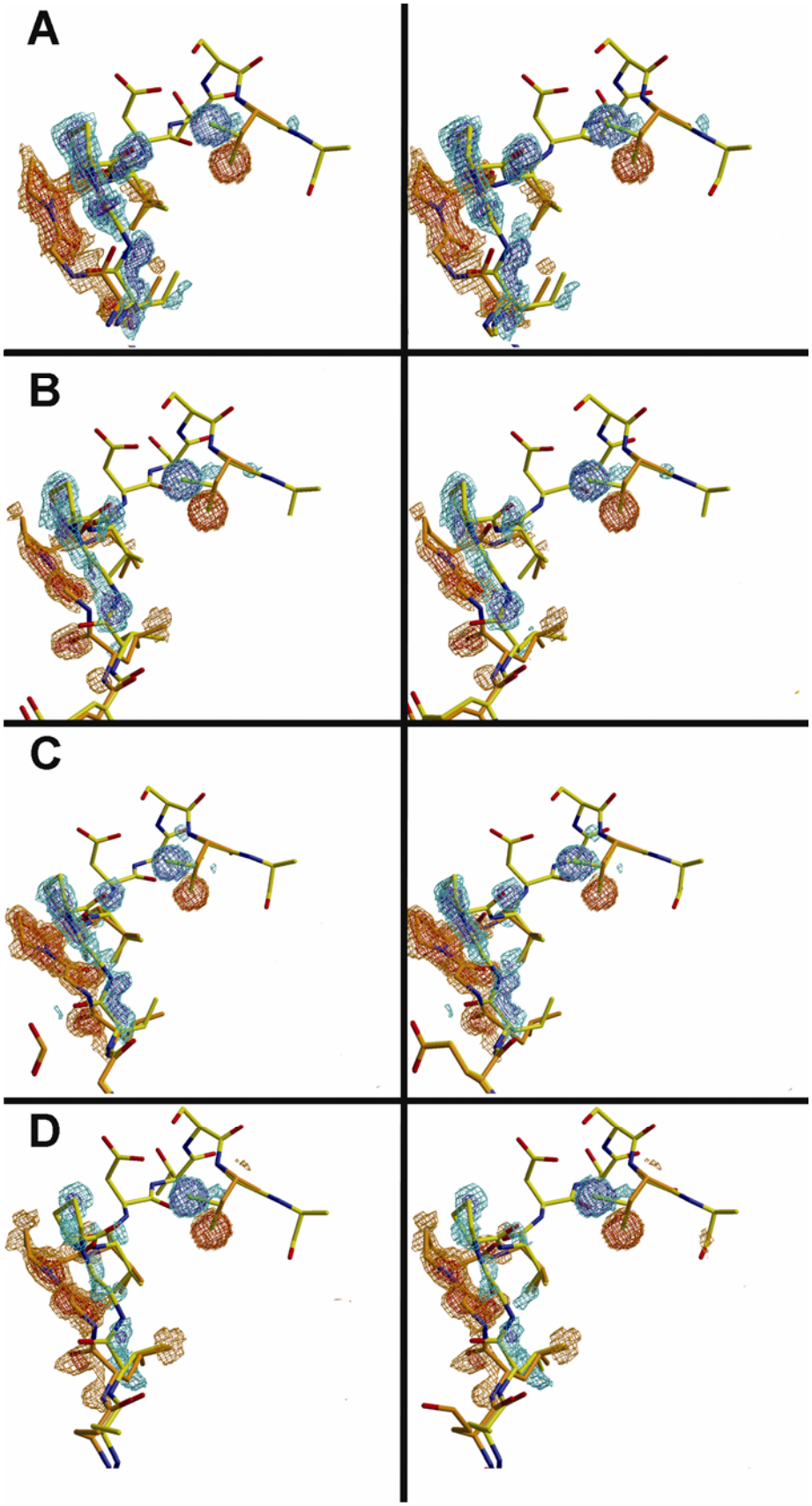
A
B
C
D

Supplemental Fig S5. SAXS data of VVD-36 dark and light states.

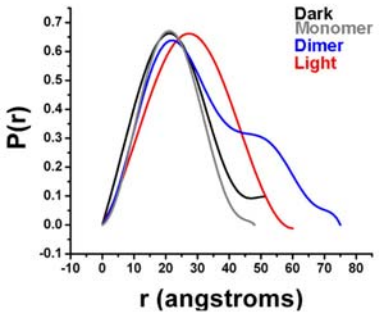

Solution electron density distributions of dark and light state VVD from SAXS. The pairwise distribution (P(r)) of electron density of the VVD dark state (black) agrees well with a theoretical distribution calculated from the monomer crystal structure (grey). In contrast, the light-state appears larger (red), but does not match the distribution expected from a closely associated dimer (blue).

Supplemental Tables

Table S1. Data Collection and Phasing Statistics

	VVD	Light	C71S	PDEVVD
Space group	P2(1)	P2(1)	P2(1)	P2(1)
Cell Dimensions (Å^3)	36.4 x 80.7 x 58.6	63.0 x 81.1 x 64.7	36.3 x 80.6 x 57.8	64.1 x 80.6 x 64.1
–angle (degrees)	95.8	90.0[3]	95.6	90.0[3]
No. residues	291	588	287	574
Cofactor	FAD	FAD	FAD	FMN
No. of water molecules	314	500	373	565
Resolution	2.0 (2.09-2.00)	1.7 (1.78-1.70)	1.8 (1.88-1.80)	2.3 (2.42-2.30)
No. unique reflections	39739	51485	28612	32764
% completeness	92.3 (66.4)	82.9 (63.6)	93.8 (74.3)	99.3 (94.5)
<I/ I>	22.56 (4.32)	13.31 (1.91)	21.64 (2.81)	25.4 (3.07)
Rmerge[1] (%)	7.2 (20.2)	10.2 (43.1)	8.4 (31.4)	7.3 (51.4)
R-factor[2] (%)	24.6 (30.1)	22.6 (32.2)	26.1 (36.0)	24.2 (27.1)
R_{free}(%)	29.3 (33.8)	24.9 (33.6)	28.2 (38.8)	27.6 (30.4)
Overall <B>	37.7	21.5	29.9	43.3
Main chain <B>	35.0	18.9	26.9	40.5
Sidechain <B>	36.3	20.8	29.3	44.3
rmsd for bonds	0.009	0.009	0.01	0.009
rmsd for angles	1.4	1.4	1.8	1.3

[1] $R_{merge} = \sum_j |I_j - \langle I \rangle| / \sum_j I_j$

[2] R-factor = $(|F_{obs}|-|F_{calc}|)/ |F_{obs}|$

[3] The light-state and PDE structures are pseudo-orthorhombic. To validate the monoclinic lattice, we repeated the refinement by assigning the crystallographic two-fold screw axis to either of the two non-crystallographic two-fold axes (the cells can be indexed with the true two-fold along any of three directions). In both cases the R-free increased ~4% percent, indicating that the additional symmetry is not crystallographic.

Table S2. FPLC Analysis of VVD-36 Variants

	Dark Elution Volume (ml)	Light Elution Volume (ml)	Apparent MW Dark (kDa)	Apparent MW Light (kDa)
Dimer	156.3	-	51.4	-
N+6 VVD-36	183.7	168.0	22.5	36.2
N-6 VVD-36	189.0	177.3	19.2	27.3
VVD-36	190.8	171.7	18.2	32.4
FLVVD	186.3	180.3	20.8	25.0
Cys71Ser	190.9	189.9	18.1	18.7
Cys71Ala	188.9	174.6	19.3	29.7
Cys71Val	186.2	169.0	20.9	35.1

References

1. C. Gradinaru, B. R. Crane, *J. Phys. Chem. B* **110**, 20073 (2006).
2. S. A. Kang, B. R. Crane, *Proc. Natl. Acad. Sci. USA* **102**, 15465 (2005).
3. S. A. Kang, K. R. Hoke, B. R. Crane, *J. Am. Chem. Soc.* **128**, 2346 (2006).
4. S. A. Kang, P. J. Marjavaara, B. R. Crane, *J. Am. Chem. Soc.* **126**, 10836 (2004).
5. A. Otwinowski, W. Minor, *Methods Enzymol.* **276**, 307 (1997).
6. J. Navaza, *Acta Crystallogr.* **A50**, 157 (1994).
7. D. E. McRee, *J. Mol. Graph.* **10**, 44 (1992).
8. A. T. Brunger *et al.*, *Acta Crystallogr.* **D54**, 905 (1998).
9. R. Fedorov *et al.*, *Biophys. J.* **84**, 2474 (2003).
10. D. I. Svergun, *J. Appl. Cryst.* **25**, 495 (1992, 1992).
11. D. I. Svergun, M. V. Petoukhov, M. H. Koch, *Biophys. J.* **80**, 2946 (2001).
12. D. I. Svergun, C. Barberato, M. H. Koch, *J. Appl. Cryst.* **28**, 768 (1995).
13. R. H. Davis, F. J. DeSerres, *Methods Enzymol.* **17A**, 79 (1970).
14. C. Schwerdtfeger, H. Linden, *The EMBO Journal* **22**, 4846 (2003).
15. N. Garceau, Y. Liu, J. J. Loros, J. C. Dunlap, *Cell* **89**, 469 (1997).